# Efficient Computation of "Stiff" Chemically Reacting Flow in Turbulent Free Jets

P.D. Thomas* and K.H. Wilson†
*Lockheed Palo Alto Research Laboratory, Palo Alto, Calif.*

**The chemically reacting flow in axisymmetric, turbulent free jets is solved numerically by a second-order accurate finite-difference scheme that is unconditionally stable with respect to the chemical rates. The transport properties are obtained from the turbulent kinetic energy model of turbulence. The momentum, energy, and turbulence model equations are solved by an explicit differencing scheme, whereas a hybrid expolcit/implicit scheme is used to solve the species conservation equations. High computational efficiency is attained by solving the equations in a natural coordinate system, and by employing the chemical element conservation principles to minimize the order of the matrix inverted to obtain the species concentrations. The scheme computes reacting jet flows in one-fifth the computer time required by any previously reported scheme.**

## Nomenclature

$C$ = mass concentration
$f$ = mole-mass ratio (moles per unit mass of mixture)
$\boldsymbol{g}$ = flow variable vector [Eq. (1b)]
$h$ = dimensionless static enthalpy (normalized by $u_e^2$)
$H$ = dimensionless total enthalpy (normalized by $u_e^2$)
$k$ = dimensionless turbulent kinetic energy (normalized by $u_e^2$)
$k_f, k_b$ = forward and backward rate constants
$K_p$ = equilibrium constant
$M$ = molecular weight (g/mole)
$\boldsymbol{n}$ = element mole-mass ratio vector [Eq. (27b)]
$p$ = pressure
$r$ = dimensionless radial coordinate (normalized by initial jet radius $r_e$)
$R$ = Universal gas constant
$T$ = temperature
$u,v$ = dimensionless velocity components in axial and radial directions, normalized by $u_e$
$u_e$ = initial jet centerline velocity
$Y$ = stretched normalized stream function [Eq. (13)]
$z$ = dimensionless axial coordinate (normalized by initial jet radius $r_e$)
$\Delta h_i^0$ = heat of formation
$\Delta F_i^0$ = Gibbs free energy
$\mu$ = dimensionless turbulent viscosity
$\rho$ = dimensionless density, normalized by $\rho_e$
$\rho_e$ = initial jet centerline density
$\tau$ = chemical relaxation time
$\psi$ = stream function
$\omega_i$ = species production rate (moles per g of mixture/sec

*Subscripts*

$e$ = initial value at jet centerline
$i$ = species index
$j$ = grid line index
$Y,r,z,\psi$ = partial derivative with respect to $Y$. $r$, $z$, or $\psi$
$\infty$ = freestream value

*Superscripts*

$'$ = derivative with respect to $z$
$n$ = integration step index
$\sim n+1$ = predicted value at step $n+1$

Presented at the AIAA 2nd Computational Fluid Dynamics Conference, Hartford, Conn., June 19-20, 1975 (no preprints, pp. 124-132 bound volume Conference papers); submitted June 20, 1975; revision received Nov. 3, 1975. This work was performed under the Lockheed Independent Research Program.

Index categories: Jets, Wakes, and Viscid-Inviscid Flow Interactions; Reactive Flows.

*Staff Scientist, Fluid Mechanics Laboratory. Member AIAA.

†Senior Staff Scientist, Fluid Mechanics Laboratory. Member AIAA.

## Introduction

THE dispersion of pollutants introduced into the atmosphere by air-breathing jet engine exhausts and the flow in afterburning rocket exhaust plumes are two problems of current interest to the scientific community. In either problem, a major part of the flowfield can be modeled as an axisymmetric turbulent, chemically reacting, free jet. A number of computer programs have been developed to obtain numerical finite-difference solutions based on this model. Examples are the programs reported by Mikatarian[1] and by Jensen and Wilson,[2] the latter of which was adapted from Patankar and Spaulding's earlier nonreacting flow program.[3] Although these programs run reasonably fast, their usefulness is marginal in certain practical applications, such as parametric studies that involve large numbers of runs, where computational efficiency is of paramount importance. The present paper describes the computational techniques that have been used in a currently operational program that computes reacting jet flows in one-fifth the computer time required by previously existing programs.

## Free-Jet Flow Equations

### Formulation

Turbulent shear flows in general are the subject of intensive research and are not yet well understood. This is particularly true of compressible, chemically reacting flows. The theoretical treatment of such flows is currently limited to phenomenological models that involve many assumptions and idealizations. The following formulation reflects the state of the art in modeling compressible, reacting, free jet flows.[4]

We consider the problem of the turbulent mixing of two chemically reacting, coaxial streams under the constraint that pressure is everywhere constant. Our attention is restricted to that portion of the flowfield where the boundary-layer approximation is valid. We introduce the further approximation of binary diffusion, i.e., the assumption that all species interdiffuse at equal rates. The diffusion flux of each species then obeys Fick's law with the same diffusion coefficient for all species.[5] Turbulent transport properties are determined from the turbulent kinetic energy (TKE) model proposed by Lee and Harsha.[6,7] This model introduces a partial differential equation for the turbulent kinetic energy $k$. Finally, we introduce, for simplicity, the assumption that the Prandtl and Lewis numbers be unity. This latter assumption can be

removed readily. Under these constraints and assumptions, the partial differential equations for a free jet can be written in the vector form below. All variables and equations that appear in the text are dimensionless (see Nomenclature).

$$\rho u g_z + \rho v g_r = r^{-1}(r\mu g_r)_r + \rho u \phi \tag{1a}$$

$$g \equiv (u, H, k, f_1, f_2, \ldots, f_i, \ldots, f_I)^T \tag{1b}$$

$$\phi \equiv u^{-1}(0, 0, \phi_k, \omega_1, \omega_2, \ldots, \omega_i, \ldots, \omega_I)^T \tag{1c}$$

where we have dispensed with the mass conservation equation because we will later introduce the von Mises transformation under which this equation is satisfied identically. These equations are subject to the boundary conditions

$$v = 0, g_r = 0 \text{ at } r = 0 \tag{2a}$$

$$v \to 0, g \to g_\infty \text{ as } r \to \infty \tag{2b}$$

and to prescribed initial conditions at some given axial position which we denote as $z = z_0$.

Under the TKE model of Lee and Harsha,[6,7] the viscosity is given by

$$\mu = \rho a_1 k / |u_r| \tag{3}$$

where $a_1$ also is a prescribed constant.

The source term for the turbulent kinetic energy represents the difference between production and dissipation[6]

$$\phi_k = \mu u_r^2/\rho - a_2 k^{3/2}/\ell \tag{4}$$

where $a_2$ is a prescribed constant, and $\ell$ is a characteristic length. In our calculations, we have used the values $a_1 = 0.3$, $a_2 = 1.75$, and have set $\ell$ equal to twice the velocity half-width of the mixing region.[7]

The source terms $\omega_i$ for the various species conservation equations (written in terms of the species mole-mass ratio $f_i = C_i/M_i$ rather than the usual species mass fraction $C_i$) are computed by summing the forward minus backward production terms for a given species over all reactions. Two-body reaction rates are prescribed in the forward direction $k_f$ and the backward rates are computed using the equilibrium constant

$$k_b = k_f (p/RT)^{-\nu}/K_p \tag{5}$$

$$K_p = \exp - \left\{ \sum_i \Delta F_i^0/RT \right\} \tag{6}$$

where $\nu = 0$ for two-body and $\nu = 1$ for three-body reactions assuming all third bodies yield the same rate.

The state equation is

$$p = \rho RT/M \tag{7a}$$

with

$$M = \left[ \sum_i f_i \right]^{-1} \tag{7b}$$

and temperature is determined from an iterative solution to the equation that defines the static enthalpy of the gas mixture

$$h = \sum_i f_i [h_i(T) + \Delta h_i^0] \tag{8}$$

The JANNAF data are used to provide the temperature-dependent values for the species enthalpy and Gibbs free energy.

**von Mises Coordinate Transformation**

We now transform to a von Mises coordinate $\psi$ defined by

$$\psi_r = \rho u r; \quad \psi_z = -\rho v r \tag{9}$$

In the von Mises coordinates, the conservation equations become

$$g_z = (\epsilon g_\psi)_\psi + \phi \tag{10a}$$

$$\epsilon = \rho u r^2 \mu \tag{10b}$$

and the boundary conditions are

$$(\epsilon g_\psi)_\psi \to 2\mu g_\psi \text{ at } \psi = 0 \tag{11a}$$

$$g \to g_\infty \qquad \text{at } \psi \to \infty \tag{11b}$$

where the arrow in Eq. (11a) indicates the substitution of terms that is needed in Eq. (10a) to obtain the equation that applies on the axis of symmetry $r = \psi = 0$.

**Natural Coordinate System**

Important advantages in both the simplicity and computational efficiency of the numerical solution can be gained by assuming the existence of a finite jet boundary $\psi = \psi_\infty(z)$ at which the dependent flow variable $g$ takes on its freestream value[3]

$$g = g_\infty \quad \text{at} \quad \psi = \psi_\infty \tag{12}$$

The boundary position must grow in the axial direction at the same rate the jet spreads by turbulent transport. For some turbulence models, the existence of such a boundary can be deduced from the mathematical properties of the governing equations.[3] This is true for both the Prandtl mixing length model and the TKE model used here, provided that, in the latter case, the freestream turbulence level is neglected ($k_\infty = 0$). For turbulence models in which the effective viscosity $\mu$ does not vanish in the freestream, as well as for laminar flow, the introduction of a finite boundary is merely a convenient approximation.

The normalized stream function $\psi/\psi_\infty(z)$ represents a "natural" lateral coordinate for the free jet, and is similar to that employed by Patankar and Spaulding.[3] Because the stream function is a strong function of the density, this coordinate is poorly suited to the problem of interest here, which involves a hot, low-density jet in a cool, relatively dense freestream. This deficiency can be overcome by employing a stretched coordinate[8]

$$Y = (1/\beta)\sinh^{-1}[(\psi/\psi_\infty)\sinh\beta] \tag{13}$$

where $\beta$ is an arbitrary stretching coefficient that may vary with axial position $x$ along the jet. We introduce a transformation of the independent variables $(z, \psi) \to (z, Y)$. The transformation maps the jet flow region $0 \le \psi \le \psi_\infty$, $z \ge z_0$ onto the unit strip $0 \le Y \le 1$, $z \ge z_0$.

The transformed governing equations and boundary conditions are

$$g_z = -Y_z g_Y + Y_\psi (\epsilon Y_\psi g_Y)_Y + \phi \tag{14}$$

$$g(z, 1) = g_\infty \tag{15a}$$

$$Y_\psi (\epsilon Y_\psi g_Y)_Y \to 2\mu Y_\psi g_Y \text{ at } Y = 0 \tag{15b}$$

where the partial derivatives of the transformation are

$$Y_\psi = (\sinh\beta)/\beta\psi_\infty \cosh\beta Y \tag{16a}$$

$$Y_z = -(1/\beta)\{(\psi'_\infty \tanh\beta Y)/\psi_\infty + \beta'[Y-(\tanh\beta Y)/\tanh\beta]\} \quad (16b)$$

To complete the formulation, we require an additional equation that specifies the motion of the boundary $\psi_\infty$.

#### Boundary Motion

The boundary $\psi_\infty(z)$ must grow at the rate the jet spreads by turbulent transport. The spreading rate is coupled to the boundary motion through Eq. (14). The latter equation applies throughout the interval $0<Y<1$, and must be satisfied in the limit as $Y\to 1$ from below. This limiting form of Eq. (14) must be consistent with the boundary condition of Eq. (15a), which implies

$$g_z(z,1)=0 \quad (17)$$

if we take the freestream to be uniform. Upon combining Eq. (17) with the limiting form of Eq. (14) and noting that $\phi$ vanishes in the uniform (nonreacting and nonturbulent) freestream, we obtain the result

$$\psi'_\infty [g_Y]_{Y=1} + \left[(\epsilon Y_\psi g_Y)_Y\right]_{Y=1} = 0 \quad (18)$$

Since $\psi_\infty$ is a scalar, whereas $g$ is a vector, Eq. (18) represents an overdetermined system of differential equations that must obey a consistency condition in order to yield a unique expression for $\psi'_\infty$. We shall see later that uniqueness follows automatically when an appropriate finite-difference approximation is employed to represent the $Y$-derivatives in Eq. (18).

## Numerical Solution

The transformed equations (14) retain the parabolic character of the original equations. Along with Eq. (18), they are to be solved numerically by forward integration in the $z$-direction, starting with prescribed initial conditions. To effect the solution, we construct a grid in the $Y$-direction with a uniform grid interval $\Delta Y = 1/J$, where $J$ is an integer. The coordinates of the grid lines are $Y_j=(j-1)\Delta Y$, $j=1,2,\ldots,J+1$. Two alternative differencing schemes are employed, depending upon whether the chemistry is stiff or is nearly frozen. In the latter case, a simple, conditionally stable explicit scheme is employed. For chemically stiff flows, a special hybrid explicit/implicit scheme is employed that is unconditionally stable with respect to the chemical production rates.

#### Fully Explicit Differencing Scheme

To advance the solution of Eq. (14) by one integration step from $z^n$ to $z^{n+1}=z^n+\Delta z$, we employ MacCormack's predictor-corrector scheme,[9] which is of second-order accuracy in both $\Delta Y$ and $\Delta z$. The scheme can be written in the form

$$\text{Predictor: } \tilde{g}_j^{n+1} = g_j^n + \Delta z (g_z)_j^n \quad (19a)$$

$$\text{Corrector: } g_j^{n+1} = \tfrac{1}{2}[g_j^n + g_j^{n+1} + (\tilde{g}_z)_j^{n+1}] \quad (19b)$$

where, in the predictor

$$(g_z)_j^n = \phi_j^n - (Y_z)_j^n (g_{j+1}^n - g_j^n)/\Delta Y + [(\epsilon Y_\psi)_{j+1/2}^n (g_{j+1}^n - g_j^n) - (\epsilon Y_\psi)_{j-1/2}^n (g_j^n - g_{j-1}^n)](Y_\psi)_j^n/(\Delta Y)^2 \quad (20a)$$

and in the corrector

$$(\tilde{g}_z)_j^{n+1} = \tilde{\phi}_j^{n+1} - (\tilde{Y}_z)_j^{n+1}(\tilde{g}_j^{n+1} - \tilde{g}_{j-1}^{n+1})/\Delta Y + [(\tilde{\epsilon}\tilde{Y}_\psi)_{j+1/2}^{n+1}(\tilde{g}_{j+1}^{n+1} - \tilde{g}_j^{n+1}) - (\tilde{\epsilon}\tilde{Y}_\psi)_{j-1/2}^{n+1}(\tilde{g}_j^{n+1} - \tilde{g}_{j-1}^{n+1})](\tilde{Y}_\psi)_j^{n+1}/(\Delta Y)^2 \quad (20b)$$

The half-integer subscripts denote the arithmetic average of values between adjacent mesh points

$$(\epsilon Y_\psi)_{j+1/2} = [(\epsilon Y_\psi)_j + (\epsilon Y_\psi)_{j+1}]/2 \quad (20c)$$

At the symmetry axis $Y=0$, where $j=1$, Eq. (20a) is replaced by

$$(g_z)_j^{n+1} = \phi_j^n - [(Y_z)_j^n - 2(\mu Y_\psi)_{j+1/2}^n](g_{j+1}^n - g_j^n)/\Delta Y \quad (20d)$$

The correct formula for $j=1$ is obtained directly from Eq. (20d) upon replacing the superscript $n$ by $\sim n+1$.

The stream-function coordinate system becomes singular at the symmetry axis $Y=\psi=0$. This is reflected in Eq. (15b) by the drastic change in the form of the lateral transport term as $\psi\to 0$ that is required to meet the symmetry boundary condition of Eq. (2a). The singular behavior requires special provisions to ensure that the difference equations (20) satisfy the physically and mathematically necessary condition that the shear stress, heat flux, and diffusion fluxes be continuous over the grid interval between $j=1$ and $j=2$. This requirement is satisfied if we define

$$\mu_{j+1/2} = (\epsilon Y_\psi)_{j+1/2}/\Delta Y \text{ for } j=1 \quad (21)$$

A unique expression for the boundary slope $\psi'_\infty$ can be obtained directly from Eq. (18) as follows. We construct a fictitious grid line $j=J+2$ located at $Y_{J+2}=1+\Delta Y$. Since this grid line lies within the freestream, we have $g_{J+2}=g_{J+1}=g_\infty$. When the $Y$-derivative terms that appear in Eq. (18) we approximated by standard second-order central differences centered about the grid line $Y_{J+1}=1$, there results the following unique scalar equation

$$\psi'_\infty = 2(\epsilon Y_\psi)_{J+1/2}/\Delta Y \quad (22)$$

The fundamental validity of this result can be verified by examining the global conservation properties of the difference equations (20). Both Eqs. (21) and (22) emerge as necessary conditions under which the difference equations satisfy, to second-order accuracy in $\Delta z$ and $\Delta Y$, the same integral conservation relations that are satisfied by the partial differential equations (14). The boundary position $\psi_\infty(z)$ is computed from difference equations that are obtained from Eqs. (19a,b) by the substitution $g_z\to\psi'_\infty, g\to\psi_\infty$.

As indicated earlier, the coordinate-stretching function in Eq. (13) is introduced to provide good spatial resolution of the low-density inner region of the jet. The inverse hyperbolic sine stretching function has proved successful in treating other flow problems with strong lateral density variations.[8] In the present application, the stretching allows one to focus the computational grid lines near the jet centerline, with the effective grid-line spacing $\Delta\psi \approx \psi_Y \Delta Y$ controlled by the magnitude of the coefficient $\beta$. The latter is computed as a continuous function of $z$ to maintain a fixed number of grid lines within the half-velocity radius of the jet. This is accomplished by constructing a differential equation for $\beta$ such that the excess velocity $u-u_\infty$ at some fixed point $Y_0\epsilon(0,1)$ remains at a predetermined constant fraction $\delta\approx\frac{1}{2}$ of the excess velocity at the jet centerline

$$u(z,Y_0) - u_\infty = \delta[u(z,0) - u_\infty]$$

Upon taking the $z$-derivative of this equation, we obtain a linear relation between $u_z(z,Y_0)$ and $u_z(z,0)$. An equation

for each of these derivatives can be obtained directly from the first component of the vector Eq. (14), evaluated successively at $Y=Y_0$ and at $Y=0$. The three equations can be manipulated to yield the following differential equation for the stretching coefficient

$$(1/\beta\tanh\beta)\,(Y_0\tanh\beta-\tanh\beta Y_0)\beta' = -(\psi'_\infty/\beta\psi_\infty)\tanh\beta - Y_0$$
$$= -(\psi'_\infty/\beta\psi_\infty)\tanh\beta Y_0$$
$$+\{2\delta[\mu Y_\zeta u_Y]_{Y=0} - [Y_\zeta(\epsilon Y_\zeta u_Y)_Y]_{Y=Y_0}\}/$$
$$[u_Y]_{Y=Y_0} \tag{23}$$

If we chose $\delta=\frac{1}{2}$ and $Y_0=(j^*-1)\Delta Y$, where $j^*$ is the greatest integer in $J/2$, then $Y_0$ coincides with the grid line $j=j^*$. The $Y$-derivatives that appear in Eq. (23) then can be evaluated by the same difference formulas employed in Eqs. (20). The differenced form of Eq. (23) is integrated simultaneously with the flow equations, and has the effect of maintaining half the grid lines within the half-velocity radius.

#### Stability

We have not performed a general stability analysis. Instead, we have simply analyzed the stability of the scheme separately for each of three simpler model equations obtained from Eq. (14) by retaining only one of the terms on the right-hand side and dropping the others.

If the convective term alone is retained ($\epsilon=\phi=0$), the stability condition is the well-known C.F.L. condition

$$\Delta z \le \Delta Y/|Y_z| \tag{24a}$$

When the turbulent transport term alone is retained ($Y_z=\phi=0$), Eq. (14) takes on the form of the transient heat-conduction equation. The stability criterion is then identical to the well-known one for explicit schemes[10]

$$\Delta z \le (\psi_Y\Delta Y)^2/2\epsilon \tag{24b}$$

When only the source term is retained ($Y_z=\epsilon=0$), Eq. (14) reduces to an ordinary differential equation. Since we are most concerned with the stability limitations associated with the species conservation equations, we restrict attention to the last $I$ components of Eq. (14) $df/dz=\omega/u$. For such a system of ordinary differential equations, the differencing scheme of Eq. (19) is equivalent to the second-order Runge Kutta scheme whose stability boundary is[11] $\Delta z \le 2u/|\lambda|_{\max}$ where $\lambda$ is an eigenvalue of the Jacobian matrix $\{\partial\omega_i/\partial f_k\}$.

The spectral radius $|\lambda|_{\max}$ can be estimated in terms of a natural matrix norm to obtain the following commonly used approximation

$$\Delta z \le u/\max_i|\partial\omega_i/\partial f_i| = u(\tau_i)_{\min} \tag{24c}$$

where we have identified the diagonal elements of the Jacobian matrix as the usual chemical relaxation time[12] $\tau_i=|\partial\omega_i/\partial f_i|^{-1}$.

We assume that the numerical solution to the full equation (14) will be stable if $\Delta z$ satisfies simultaneously the stability criteria of Eqs. (24). Thus, we use the formula

$$\Delta z \le \left[|Y_z|/\Delta Y + 2\epsilon/(\psi_Y\Delta Y)^2 + u^{-1}(\tau_i)^{-1}_{\min}\right]^{-1} \tag{25}$$

A stepsize $\Delta z$ equal to 90% of the minimum value calculated from Eq. (25) for all mesh points has been found to maintain stability.

In nonreacting flows ($\omega_i=0$), changes in the flow variables $g$ as a function of axial position $z$ are governed by turbulent transport, and the second term inside the brackets on the right-hand side of Eq. (25) is dominant. That term remains dominant in chemically reacting flows where the freestream pressure is sufficiently low that the chemical rates $\tau_i^{-1}$ are small (nearly frozen flow). The stability criterion of Eq. (25) then reduces to Eq. (24b). Even with this stepsize restriction, the overall computational efficiency of the explicit scheme is high because the stable stepsize $\Delta z$ increases with the square of the "jet width" $\psi_\infty$ as the jet spreads during the course of the calculation.

However, when one or more reactions approach local equilibrium, the last term inside the brackets in Eq. (25) is dominant. The fully explicit differencing scheme becomes inefficient because it requires a stepsize much smaller than that which governs the axial variations in the flow variables $g$ caused by spreading of the jet by turbulent transport. Computational efficiency is possible only with a differencing scheme that is free of stability criteria associated with this stiffness near local equilibrium conditions.

#### Hybrid Explicit/Implicit Differencing Scheme

A widely used approach for the numerical treatment of "stiff" systems of equations involves the use of some sort of implicit differencing scheme. Arguments have been given in the preceding paragraph to the effect that the explicit scheme is computationally efficient for those flow variables whose axial variation is primarily caused by the turbulent transport that is responsible for lateral spreading of the jet. Therefore, we continue to use the explicit scheme to compute the first three components of the vector $g$ in Eq. (14), namely, $u$, $H$, and $k$. The chemical species conservation equations embodied in the last $I$ components of Eq. (14) obey the equation

$$f_z = -Y_\zeta f_Y + Y_\psi(\epsilon Y_\psi f_Y)_Y + \omega/u \tag{26a}$$

$$f=(f_1,f_2,\ldots,f_i,\ldots,f_I)^T, \tag{26b}$$

$$\omega=(\omega_1,\omega_2,\ldots,\omega_i,\ldots,\omega_I)^T \tag{26c}$$

and will be treated with a special hybrid explicit/implicit scheme. Before introducing the scheme, we shall reformulate the chemistry problem in a way that enables us to take full advantage of the explicit part of the calculation by making use of the chemical element conservation relations.

##### *Element Conservation*

The $I$ components of Eq. (26) form a complete set for the determination of the individual mole-mass ratios $f_i$. That is, $f$ is a basis for the vector space of solutions to Eq. (16). However, the $f_i$ obey a set of well-known linear relations that express the conservation of chemical elements. If the $I$ individual species are composed of $L$ distinct chemical elements, then these relations can be written in the vector form

$$Vf=n \tag{27a}$$

where

$$n=(n_1,n_2,\ldots,n_\ell,\ldots,n_L)^T \tag{27b}$$

is a vector whose compound $n_\ell$ represents the mole-mass ratio of chemical element $\ell$, and

$$V=\{\nu_{\ell i}\} \tag{27c}$$

is an $L\times I$ matrix whose elements are integers such that $\nu_{\ell i}$ is the number of atoms of chemical element $\ell$ that are contained in a molecule of species $i$.

If we premultiply Eq. (26a) by $V$, we find that $n$ satisfies a

homogeneous equation, as first pointed out by Lees.[5]

$$n_z = -Y_z n_Y + Y_\psi(\epsilon Y_\psi n_Y)_Y \tag{28}$$

The vector $V\omega = 0$ vanishes because each of its components represents physically the net chemical production rate of an element, and elements are not transmuted by chemical processes.

Equation (28) is valid only under the binary diffusion approximation. As a further consequence of that approximation, we can construct the solution to the vector Eq. (28) by solving a single scalar equation of the same form. This can be demonstrated as follows. The boundary conditions on $n(z,Y)$ in Eq. (28) are $n(z,1) = n_\infty$ and a symmetry condition at $Y = 0$. The initial conditions for each component $n_\ell$ can be written in terms of the normalized transverse distribution at the initial station $z = z_0$

$$[n_\ell(z_0,Y) - n_{\ell\infty}]/(n_{\ell e} - n_{\ell\infty}) = \mathfrak{F}_\ell(Y)$$

where $n_{\ell e} = n_\ell(z_0,0)$ is the initial centerline value. If we define

$$\alpha_\ell(z,Y) = [n_\ell(z,Y) - n_{\ell\infty}]/(n_{\ell e} - n_{\ell\infty})$$

then each $\alpha_\ell$ satisfies a linear, homogeneous scalar equation that is identical in form to Eq. (28) with homogeneous boundary conditions and the initial condition $\alpha_\ell(z_0,Y) = \mathfrak{F}_\ell(Y)$. Each $\alpha_\ell$ then satisfies precisely the same initial-boundary value problem, provided that the initial distribution $\mathfrak{F}_\ell(Y)$ is the same for every chemical element $\ell$. This will always be the case when the initial distribution is obtained from an independent solution (under the binary diffusion approximation) for the reacting flow in the near-field region between the jet exhaust exit plane and our initial data plane $z = z_0$. Since the boundary-value problem for $\alpha_\ell$ is independent of $\ell$, all $\alpha_\ell$'s are identical and it follows that

$$n = \alpha n_e + (1-\alpha) n_\infty \tag{29}$$

where $\alpha$ obeys a scalar equation identical in form to Eq. (28), and can be computed efficiently with the explicit differencing scheme introduced earlier. Thus there is considerable advantage to be gained by employing a basis that consists in part of the components of $n$. In general, $L \le I$, so that the components of $n$ do not form a basis in themselves. To complete the basis, we may select from $f$ a subspace $y$ of dimension $M = I - L$.

$$y = (y_1,\ldots,y_m,\ldots,y_M)^T \tag{30a}$$

This corresponds to a partitioning of the matrix $V$ into an $L \times L$ square matrix $A$ and an $L \times M$ rectangular matrix $B$ such that

$$Vf = Ax + By = n \tag{30b}$$

$$A = \{\nu_{\ell j}\}\ \ell = 2,1,\ldots,L, j = M+1, M+2,\ldots,I \tag{30c}$$

$$B = \{\nu_{\ell m}\}\ \ell = 1,2,\ldots,L, m = 1,2,\ldots,M \tag{30d}$$

$x$ is an $L$-dimensional vector consisting of those compoments of $f$ that are not selected as components of $y$ in filling out the basis. One sees immediately from Eq. (30b) that the $I$-dimensional vector $(y,n)^T$ is a proper basis if and only if $A$ is nonsingular, for then Eq. (30b) can be solved directly for the remaining mole-mass ratios

$$x = A^{-1}n - A^{-1}By \tag{31}$$

Thus, the selection of $y$ is arbitrary within rather wide limits.

The change of basis allows us to construct the solution for $f$ by solving a relatively small set of $M$ potentially stiff species conservation equations

$$y_z = -Y_z y_Y + Y_\psi(\epsilon Y_\psi y_Y)_Y + \omega/u \tag{32}$$

where $\omega = (\omega_1,\ldots,\omega_m,\ldots,\omega_M)^T$ is a vector whose $m$th component represents the production rate of species $y_m$. The remaining components of $f$ can then be obtained directly from Eqs. (29) and (31).

*Hybrid Differencing Scheme*

To integrate Eq. (32), we employ a modified predictor-corrector scheme. The predictor is fully explicit, but treats the species as if they were chemically inert ($\omega = 0$). The chemical production-rate term $\omega$ is differenced in implicit fashion in the corrector, but the convection and turbulent diffusion terms are again differenced in an explicit fashion. The predictor is similar to Eq. (19a), with the $Y$-derivative terms differenced as in Eqs. (20a) and (20d). However, to avoid the accumulation of roundoff errors, we write the predictor in terms of the predicted change in $y$ over the step

Predictor:

$$(\Delta\tilde{y})_j^{n+1} = \Delta z\,\mathfrak{L}_Y^n(y) \tag{33a}$$

$$(\Delta\tilde{y})_j^{n+1} \equiv \tilde{y}_j^{n+1} - y_j^n \tag{33b}$$

where $\mathfrak{L}_Y^n$ represents the explicit difference operator consisting of the last two terms on the right-hand side of Eq. (20a).

In the corrector, all terms containing $Y$-derivatives are differenced explicitly in the same fashion as done in Eq. (20b), whereas the species production rate term $\omega$ is treated by the Crank-Nicholson implicit scheme—a scheme which Lomax and Bailey[11] have suggested as optimum for one-dimensional, inviscid, stiff-reacting flows

$$(\Delta y)_j^{n+1} = \frac{\Delta z}{2}\left[\mathfrak{L}_Y^n(y) + \tilde{\mathfrak{L}}_Y^{n+1}(\tilde{y}^{n+1}) + \left(\frac{\omega}{u}\right)_j^n + \left(\frac{\omega}{u}\right)_j^{n+1}\right] \tag{34a}$$

$$\Delta y_j^{n+1} \equiv y_j^{n+1} - y_j^n \tag{34b}$$

where $\tilde{\mathfrak{L}}_Y^{n+1}$ represents the explicit difference operator consisting of the last two terms on the right-hand side of Eq. (20b).

Because the differential equations for $u$, $H$, and $n$ are not coupled to Eq. (32), they may be solved to obtain $u^{n+1}$, $h^{n+1}$, and $n^{n+1}$ before starting the corrector step of Eq. (34) for the species equations (32). Hence

$$\omega_j^{n+1} = \omega(y_j^{n+1}, n_j^{n+1}, h_j^{n+1})$$

and the corrector Eq. (34) represents a coupled system of nonlinear algebraic equations for

$$(y_m)_j^{n+1} m = 1,\ldots,M$$

To avoid an iterative solution to Eq. (34a), we employ a local linearization of the nonlinear term[11]

$$\omega(y_j^{n+1}, n_j^{n+1}, h_j^{n+1}) = \omega[y_j^n, n_j^{n+1}, h_j^{n+1}) + \mathfrak{J}(\Delta y)_j^{n+1} + \ldots$$

where $\mathfrak{J}$ is the Jacobian matrix evaluated at $y_j^n$, $n_j^{n+1}$, $h_j^{n+1}$

$$\mathfrak{J} = \left[\frac{d\omega}{dy}\right]_{y^n, n^{n+1}, h^{n+1}} = \left\{\frac{\partial\omega_i}{\partial y_m}\right\} \tag{35}$$

We also use the predictor Eq. (33a) to eliminate $\mathfrak{L}_Y^n(y)$ from Eq. (34a).

The final form of the corrector is then‡

$$\text{Corrector: } [\mathcal{I} - (\Delta z/2u_j^{n+1})\mathcal{J}](\Delta y)_j^{n+1} =$$

$$\frac{1}{2}(\Delta \bar{y})_j^{n+1} + \frac{\Delta z}{2}[\bar{\mathcal{E}}_Y^{n+1}(y) + (\omega/u)_j^n$$

$$+ \omega(y_j^n, n_j^{n+1}, h_j^{n+1})/u_j^{n+1}] \tag{36}$$

where $\mathcal{I}$ is the unit matrix. The elements of the Jacobian matrix of Eq. (35) are calculated numerically by a finite-difference approximation similar to that employed by Lomax and Bailey.[11]

The change of basis effected by making use of the element conservation relations drastically reduces both the number of elements in the Jacobian matrix that must be computed, and the order of the matrix $[\mathcal{I} - (\Delta z/2u_j^{n+1})\mathcal{J}]$ that must be inverted to obtain the solution of Eq. (36). Furthermore, the coefficient matrices in Eq. (31) for the remaining species $x$ are constant matrices and need not be recalculated at each integration step. The net result yields a very substantial reduction in computer time below that which would be required if the hybrid explicit/implicit scheme were employed to integrate Eq. (26) directly.

Extensive numerical tests of the hybrid scheme have shown that roundoff errors incurred in solving Eq. (36) occasionally can lead to numerical instabilities unless some care is exercised in the selection of the base species $y$. It is recommended that the latter be chosen so that none of the elements of the constant matrix $A^{-1}B$ exceeds unity in absolute value. This is easily accomplished by inspection of the matrix $V$, and insures that roundoff errors in the computed base species $y$ are not amplified into larger errors in the derived species $x$.

*Stability and Step Control*

The well-known unconditional stability of the Crank-Nicholson scheme suggests that the hybrid scheme should be free of stability criteria associated with the chemical rates. This has been partially confirmed by a linear stability analysis of the scheme as applied to the simplified model equations obtained from Eq. (32) by dropping either the diffusion term or the convective term. If the diffusion term is omitted ($\epsilon = 0$), the stability condition is identical to that given in Eq. (24a) and arises from the explicit differencing of the convective term. Similarly, if the convective term is omitted from Eq. (32) by setting $Y_z = 0$, the stability condition is identical to Eq. (24b). For the full equation (32), we have employed the heuristic stability criterion given by Eq. (25) with the last term omitted, and have encountered no evidence of instability.

Nevertheless, as is usually the case with implicit schemes, an independent stepsize control is desirable to ensure that the truncation error of the scheme does not induce inaccuracies in the computed species concentrations. The stability criterion Eq. (25) (with the last term omitted) effectively limits that part of the truncation error associated with convection and turbulent diffusion, but does not account for the chemical processes that are dominant in highly nonequilibrium regions of the flowfield. To maintain accuracy in such regions, we use Eq. (25) to determine the size of the first step. Thereafter, we monitor at each step the maximum fractional change that took place in any of the $f_i$ during the step $\Delta z^n$

$$\delta = \max_{ij} |f_{i,j}^{n+1} - f_{i,j}^n| / f_{i,j}^n \tag{37}$$

‡We have also used a variant of this scheme in which the explicit term $(\omega/u)_j^n$ is shifted from the corrector Eq. (36) to the predictor Eq. (33). The latter variant has a smaller truncation error, but appeared to be less stable in some test calculations.

The solution for that step is considered to be of adequate accuracy if $\delta \leq \epsilon$, where $\epsilon$ is some a priori bound. On the other hand, it is desirable that $\delta$ for the next step should be reasonably close to $\epsilon$ to maintain computational efficiency without sacrificing accuracy. Thus, we estimate an accuracy-limited value for the size of next step as proportional to the ratio $\epsilon/\delta$, provided that the ratio is not too greatly different from unity

$$\Delta z_{\text{acc}}^{n+1} = \begin{cases} (\epsilon/\delta)\Delta z^n & \text{if } 0.5 \leq \epsilon/\delta \leq 1.5 \\ 0.5\Delta z^n & \text{if } \epsilon/\delta < 0.5 \\ 1.5\Delta z^n & \text{if } \epsilon/\delta > 1.5 \end{cases} \tag{38}$$

To avoid violating the stability criteria associated with the explicit part of the calculation, the actual size of the next step is chosen as

$$\Delta z^{n+1} = \min\{\Delta z_{\text{acc}}^{n+1}, \Delta z_{\text{stable}}^{n+1}\}$$

where $\Delta z_{\text{stable}}$ is given by Eq. (25) with the last term omitted. Test calculations have indicated that a value for $\epsilon$ of the order of 0.1 yields accurate solutions.

## Applications

### Incompressible Flow

The validity of the computational approach based on a natural coordinate system has been verified in tests on problems with known solutions. As an example, we have computed the flow in an incompressible jet issuing into a quiescent freestream. Tollmein has obtained an exact self-similar solution to this problem[13] under the Prandtl Mixing Length hypothesis in which the turbulent viscosity is given by $\mu = \rho \ell_m^2 |u_r|$ where the mixing length $\ell_m$ is proportional to the jet width. The self-similar solution is valid asymptotically at large $z$. Our numerical solution was started with a thin mixing region at the outer edge of a uniform potential jet core and employed ten grid intervals over the entire jet width ($J = 10$). A self-similar-similar velocity profile develops shortly after the mixing region envelops the potential core. The computed profile at $z = 100$ agrees well with the exact solution, as show in Fig. 1.

### Compressible Chemically-Reacting Flow

Presented below are computed results for two representative cases of reacting flow in large liquid rocket exhaust jets

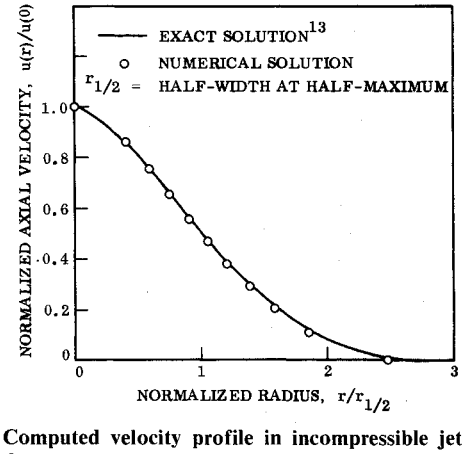


**Fig. 1 Computed velocity profile in incompressible jet at $z = 100$ compared to exact solution.**

**Table 1 Reaction set**

| | |
|---|---|
| $H+O_2$ | $\rightleftarrows OH+O$ |
| $O+H_2$ | $\rightleftarrows OH+H$ |
| $H_2+OH$ | $\rightleftarrows H+H_2O$ |
| $OH+OH$ | $\rightleftarrows H_2O+O$ |
| $CO+OH$ | $\rightleftarrows CO_2+H$ |
| $O+O+M$ | $\rightleftarrows O_2+M$ |
| $H+H+M$ | $\rightleftarrows H_2+M$ |
| $O+H+M$ | $\rightleftarrows OH+M$ |
| $OH+H+M$ | $\rightleftarrows H_2O+M$ |
| $CO+O+M$ | $\rightleftarrows CO_2+M$ |

**Table 2 Initial conditions**

| Case | 1 | 2 |
|---|---|---|
| Altitude (km) | 30 | 0 |
| $r_e$(m) | 6.32 | 0.753 |
| $T_e$(K) | 1300 | 1900 |
| $u_e$(km/sec) | 2.5 | 2.62 |
| $u_\infty$(km/sec) | 1.0 | 0.05 |

in a coflowing airstream. The cases are for a TITAN – II rocket which uses an amine fuel, and therefore has a substantial concentration of $N_2$ in the exhaust. The turbulent viscosity was computed from the TKE model. The computations included a set of 10 elementary reactions among the 8 active species—$O_2$. O, $H_2$, H, OH, $H_2O$, CO, and $CO_2$ and one inert species, $N_2$. The reactions are listed in Table 1. The forward reaction rates were taken from Ref. 14.

The numerical solutions employed ten grid intervals and were started at $z=0$ with a thin mixing region at the outer edge of a uniform jet core. The initial chemical composition in the core was specified arbitrarily, with no attempt to start with the correct equilibrium composition corresponding to the initial temperature and pressure. The base species comprising the vector $y$ were selected as H, O, OH, $H_2$, and CO. The remaining initial conditions for each of the three computed cases are listed in Table 2. Case 1 was selected at a sufficiently high altitude to allow comparison of the results computed by the hybrid differencing scheme with those of the fully explicit scheme without incurring an excessive computer run time for the explicit scheme. The other case was computed with the hybrid scheme only. The computed results are displayed in Figs. 2-5.

Figure 2 shows a comparison of the species concentration distributions along the jet centerline as computed with both schemes. Those computed by the hybrid scheme are in excellent agreement with those of the explicit scheme, and were

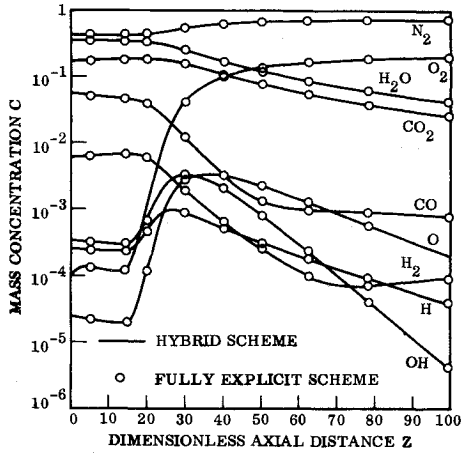


**Fig. 2 Comparison of species concentration distributions along jet centerline computed with fully expilcit scheme and with hybrid explicit/implicit scheme. Case 1, 30-km altitude.**

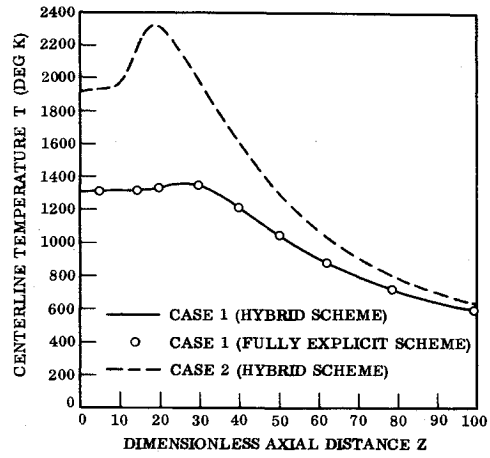


**Fig. 3 Computed temperature distributions along jet centerline for Case 1 (30-km altitude) and Case 2 (sea level altitude).**

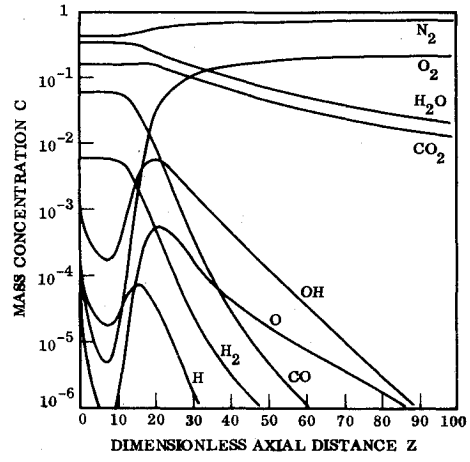


**Fig. 4 Computed species concentration distributions along jet centerline for Case 2 (sea level altitude). Hybrid scheme.**

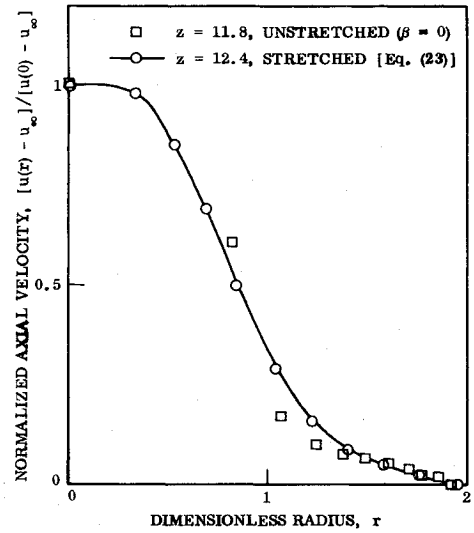


**Fig. 5 Comparison of velocity profiles computed for Case 1 with unstretched stream function coordinate ($\beta=0$) and with stretched coordinate ($\beta>0$).**

obtained in 1.2 min of computer time on the UNIVAC 1110. The run time for the explicit scheme was a factor of 10 longer. A similar comparison of the jet centerline temperature distributions computed with the two schemes is given in Fig. 3.

The latter figure also shows the centerline temperature distribution for Case 2 (sea level altitude). The corresponding species concentration distributions are displayed in Fig. 4. The UNIVAC 1110 computer run time was 1.5 min for Case 2 using the hybrid scheme.

In summary, a technique has been developed for efficiently calculating "stiff" nonequilibrium turbulent free jet flows in a rather modest amount of computer time. The technique employs a widely used, second-order accurate, explicit finite-difference scheme for solving the momentum, energy, and turbulence model equations. On the other hand, the species conservation equations are solved with a newly developed hybrid explicit/implicit differencing scheme that is unconditionally stable with respect to the chemical rates. High overall computational efficiency is achieved by employing a natural coordinate system in concert with a new procedure that invokes the element conservation laws. The procedure takes full advantage of the relative simplicity and speed of an explicit algorithm by employing an explicit integration of the element pseudo-concentration equations to minimize the order of the matrix that must be inverted to solve the species conservation equations when the production rate terms are differenced in an implicit fashion.

## References

[1]Mikatarian, R.R., Kau, C.J., and Pergament, H.S., "A Fast Computer Program for Nonequilibrium Rocket Plume Predictions," Air Force Rocket Propulsion Laboratory, Edwards AFB, Calif., AFRPL-TR-72-94, Aug. 1972.

[2]Jensen, D.E. and Wilson, A.S., "Predicting of Rocket Exhaust Flame Properties," *Combustion and Flame,* Vol. 25, Aug. 1975, pp. 43-55.

[3]Patankar, S.V. and Spaulding, D.B., "A Finite-Difference Procedure for Solving the Equations of the Two-Dimensional Boundary Layer, *International Journal of Heat Mass Transfer,* Vol. 10, Sept. 1967, pp. 1389-1411.

[4]Bushnell, D.M., "Calculation of Turbulent Free Mixing-Status and Problems," *Proceedings of the Langley Working Conference on Free Turbulent Shear Flows,* NASA Langley Research Center, Vol. I, 1972, pp. 1-10.

[5]Lees, L., "Convective Heat Transfer with Mass Addition and Chemical Reaction," *Combustion and Propulsion, Third AGARD Colloquium,* M.W. Thring, et al., eds., Pergamon Press, New York, 1958, pp. 451-498.

[6]Lee, S.C. and Harsha, P.T., "Use of Turbulent Kinetic Energy in Free Mixing Studies," *AIAA Journal,* Vol. 8, June 1970, pp. 1026-1032.

[7]Harsha, P.T. and Lee, S.C., "Analysis of Coaxial Free Mixing Using the Turbulent Kinetic Energy Methods," *AIAA Journal,* Vol. 9, Oct. 1971, pp. 2063-2066.

[8]Thomas, P.D., Vinokur, M., Bastianon, R.A., and Conti, R.J., "Numerical Solution for Three-Dimensional Inviscid Supersonic Flow," *AIAA Journal,* Vol. 10, July 1972, pp. 887-894.

[9]MacCormack, R.W., *The Effect of Viscosity in Hypervelocity Impact Cratering,* AIAA Paper 69-354, Cincinnati, Ohio, 1969.

[10]Richtmeyer, R.D., *Difference Methods for Initial-Value Problems,* Interscience Publishers, New York, 1957, p. 13.

[11]Lomax, H. and Bailey, H.E., *A Critical Analysis of Various Numerical Integration Methods for Computing the Flow of a Gas in Chemical Nonequilibrium,* TN D-4109, 1967, NASA.

[12]Vincenti, W.G. and Kruger, C.H., *Introduction to Physical Gas Dynamics,* John Wiley and Sons, New York, 1965, p. 236.

[13]Schlichting, H., *Boundary Layer Theory,* 1st Edition, McGraw-Hill, New York, 1955, p. 501.

[14]Pergament, H.S. and Jensen, D.E., "Influence of Chemical Kinetic and Turbulent Transport Coefficients on Afterburning Rocket Plumes," *Journal of Spacecraft,* Vol. 8, June 1971, pp. 643-649.